Available online at www.sciencedirect.com
SCIENCE DIRECT®
Catalysis Today 93–95 (2004) 651–657
CATALYSIS TODAY
www.elsevier.com/locate/cattod

Preparation of CdS–SiO_2 core-shell particles and hollow SiO_2 spheres ranging from nanometers to microns in the nonionic reverse microemulsions

Fei Teng [a,b], Zhijian Tian [b], Guoxing Xiong [a,*], Zhusheng Xu [b]

[a] *State Key Laboratory of Catalysis, Dalian Institute of Chemical Physics, Chinese Academy of Sciences, PO Box 110, Dalian 116023, China*
[b] *Department of Natural Gas Chemistry and Applied Catalysis, Dalian Institute of Chemical Physics, Chinese Academy of Sciences, Dalian 116023, China*

Available online 6 August 2004

Abstract

Monodispersed CdS–SiO_2 core-shell particles ranging from nanometers (30–100 nm) to micrometers (1.5–2 μm) were prepared in situ in the nonionic reverse microemulsions. After treating the core-shell particles with concentric nitric acid, the hollow silica spheres were obtained correspondingly. The particles were characterized by transmission electron microscope (TEM), selected area electron diffraction (SAED), scanning electron microscope (SEM), X-ray fluroscence (XRF), X-ray powder diffraction (XRD), nitrogen (N_2) physiadsorption, etc. The study shows that the core size and shell thickness could be tuned simply by controlling the addition amount of the reactants and the addition way; that through further processing (e.g. grafting other functional molecules on the particle surface), advanced materials could be prepared; and that the hollow silica spheres could be potentially used as a novel class of catalyst supports.

Keywords: CdS–SiO_2; Core-shell particles; Hollow silica; Nanoparticles; Microspheres

1. Introduction

The preparation of the core-shell composites is currently an attractive area of researches due to their great potential applications in the areas of electronics, photonics, catalysis, and nanotechnology [1–3]. Various technologies were used to synthesize the core-shell materials. Generally, the core-shell composites are synthesized either by direct surface reaction/precipitation or by layer-by-layer (LBL) self-assembly approaches [4–6]. One of the main challenges is how to obtain uniform and controllable structure. However, because of the very sensitive condensation/polymerization conditions for the molecular precursors, or the tendency to aggregation for the nanoparticles, it is very difficult to control the core size and shell thickness precisely. The hollow spheres could be obtained through treating the core-shell composites by calcining or chemistry- or photo-etching methods [4,5,7]. The hollow particles could be used as fillers, coatings, capsule agents and catalyst supports, etc., because they possess lower density and excellent optical properties [8–10]. Recently, silica-coated luminescent semiconductor nanocrystals (e.g., cadmium sulfide) widely used as excellent photocatalysts and optoelectronic devices, have received great attention [11–15]. The shell of silica could enhance photochemical stability of the nanocrystals and increase quantum yields of nanocrystals. The CdS–SiO_2 core-shell nanocomposites could be extended to use as biocompatible labels because of biocompatibility of the silica shell [16–18], and hollow silica sphere could be used as novel support of catalyst because of its high surface area and low weight. Typically, monodispersed silica particles are synthesized by the Stöber [19] and microemulsion methods [20–23].

In this report, monodispersed CdS–SiO_2 core-shell composites and hollow silica spheres ranging from nanometers to micrometers have been synthesized by reverse microemulsion technology. The CdS core size and the shell thickness could be easily tuned by altering the addition amount and

* Corresponding author. Tel.: +86-411-467-1991; fax: +86-411-469-4447.
E-mail address: gxxiong@dicp.ac.cn (G. Xiong).

0920-5861/$ – see front matter © 2004 Elsevier B.V. All rights reserved.
doi:10.1016/j.cattod.2004.06.125

addition ways of the reactants. The particles were characterized by TEM, SAED, XRD, N_2 physiadsorption, XRF, etc.

2. Experimental

2.1. Determination of the single-phase reverse microemulsion region

In the experiment, all the chemicals were analytical grade and used without purification. Tetraethyl orthosilicate (TEOS, $Si(OEt)_4$) (SiO_2 weight ratio $\geq$ 28.5%) was purchased from Beijing Yili Chem. Com. (China); the other chemicals were purchased from Shenyang Chem. Com. (China).

Polyoxyethylene (7) octyl phenyl alcohol ether (NP-7, $C_8H_{17}C_6H_4O(C_2H_4O)_7H$), *n*-butanol, cyclohexane and aqueous solution were used as surfactant, cosurfactant, continuous phase and dispersed phase, respectively. The titration method was used to determine the reverse microemulsion region on base of the variations from transparence to opaque. Typically, a measured amount of surfactant and cosurfactant with weight ratio of 2:1 were dissolved in cyclohexane. The organic phase was titrated with the aqueous solution ($Cd(NO_3)_2$ or Na_2S or NH_4OH) under stirring gently. When the mixture changed from transparent to opaque, the end point was reached. The measurement results and the sketch partial phase diagram of the pseudoternary system were given in Table 1 and Fig. 1, respectively.

2.2. The preparation procedure

In the experiment, three microemulsions were used, and the reverse microemulsion system consisted of NP-7, *n*-butanol, cyclohexane and aqueous phase. Three microemulsion systems contained the same compositions but different aqueous phases: 0.2 mol l^{-1} $Cd(NO_3)_2$ solution, 0.2 mol l^{-1} Na_2S solution and 25 wt.% NH_4OH solution, respectively. The $Cd(NO_3)_2$-, Na_2S- and NH_4OH-containing microemulsions were designed as ME-1, ME-2 and ME-3, respectively. To guarantee the three systems stable, the

Table 1
The compositions of ME-1 or ME-2 and ME-3

Point	Composition (W:S:CS:O (g/g))	ME-1	ME-2	ME-3
A	1.4:1.7:0.8:10.0	+	+	−
B	2.4:1.7:0.8:10.0	−	−	−
C	2.1:4.3:2.3:10.0	+	+	+
D	3.5:4.3:2.3:10.0	+	+	−
E	5.6:4.3:2.3:10.0	−	−	−
F	3.5:10.0:5.0:10.0	+	+	−
G	6.4:10.0:5.0:10.0	−	−	−

+: stable and transparent; −: unstable and opaque; W: aqueous phase, S: surfactant, CS: cosurfactant, O: oil phase; ME-1: $Cd(NO_3)_2$-containing microemulsion; ME-2: Na_2S-containing microemulsion; ME-3: NH_4OH-containing microemulsion.

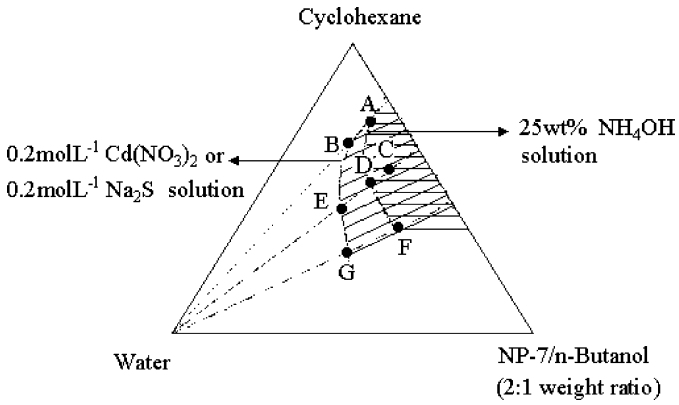

Fig. 1. Sketch pseudoternary phase diagram of aqueous solution/NP-7/*n*-butanol/cyclohexane at 25 °C.

weight ratios of aqueous phase, NP-7, *n*-butanol and cyclohexane were kept at 11:23:12:53, basing on the point C (in Fig. 1).

In order to prepare the CdS–SiO_2 core-shell particles, ME-1 was mixed with ME-2 with equal volumes under stirring gently. After ageing for 2 h, ME-3 and TEOS were added dropwise. After ageing for 24 h, acetone was added to demulsify the system, and the particles were recovered by high-speeded centrifugation. To remove the impurity ions and surfactant molecules, the particles were washed with water and alcohol at least for five to six times in sequence, respectively, and then dried in vacuum at 60 °C for 12 h. Fig. 2 gives the sketch diagram of the preparation procedure. In order to obtain the larger cores, seeding growth procedure was carried out. The small CdS seeds were firstly prepared by mixing a small amount of ME-1 and ME-2. After an appropriate interval for seeds maturation, a definite amount of ME-1 and ME-2 were further added, i.e. repeating Step 1 (in Fig. 2). The small CdS particles grew up into the desired size gradually. The similar procedure was used to control the thickness of SiO_2 shell. Firstly, a small amount of ME-3 and TEOS were added to form the thin shell; and then, a definite amount of ME-3 and TEOS were added. The thickness of silica shell was controlled through adjusting the addition amount of TEOS, i.e. repeating the Step 2 (in Fig. 2).

To obtain the hollow SiO_2 spheres, the composite samples were redispersed in water to form slurry. The concentric nitric acid was added slowly to remove the cores. The preparation procedure of the hollow SiO_2 spheres is also described in Fig. 2.

2.3. Characterization

Transmission electron microscopy (TEM) images and selected area electron diffraction (SAED) patterns were taken with a JEOL model 200CX transmission electron microscope, using an accelerating voltage of 200 kV. The samples were deposited on a thin amorphous carbon film supported by copper grids from ultrasonically processed ethanol suspension of the particles. The hollow particle morphology

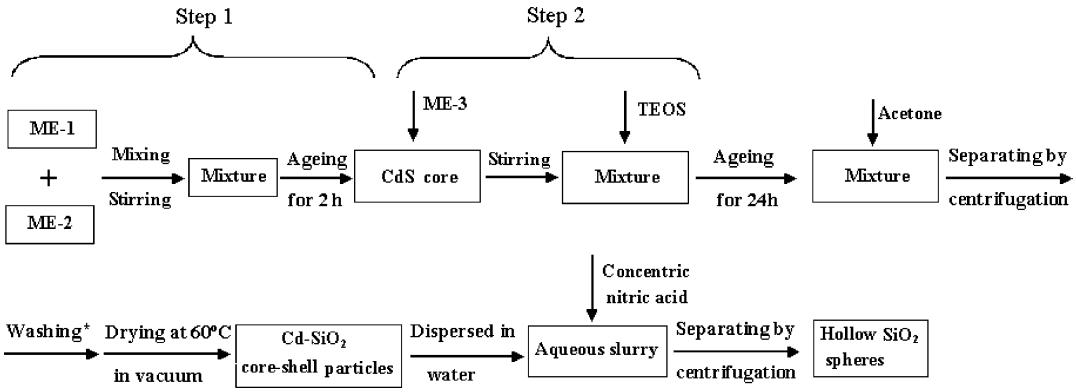

Fig. 2. The sketch diagram of the preparation procedure. Notes: ME-1: $Cd(NO_3)_2$ solution-containing microemulsion; ME-2: Na_2S solution-containing microemulsion; ME-3: NH_4OH solution-containing microemulsion; TEOS: $Si(OEt)_4$; *Washing with water and ethanol in sequence to obtain a large core, repeating Step 1; to obtain a thick shell, repeating Step 2.

was observed with scanning electron microscopy (SEM) on a JSM840 scanning electron microscope. Nitrogen (N_2) adsorption analysis was performed on a Micromeritics ASAP2010 gas adsorption analyzer, operated at 77 K and $<10^{-4}$ bar. Surface area was determined using BET method. Elemental analysis was performed on a PHLIPS Magix X-ray fluorescence (XRF) analyzer. Samples were transferred via pipet into a quartz cuvette for analysis. The discharge frequency of the fluorimeter is the same as the line frequency of 60 Hz, and the average lamp energy output is 10 W. A slit width of 10 nm was utilized in all experiments. The samples were characterized by X-ray powder diffraction (XRD) patterns using a Rigaku D/MAX-RB X-ray powder diffractometer with graphite monochromatozed Cu Kα radiation ($\lambda = 1.54178$ Å), operating at 40 kV and 50 mA, scanning rate at 5° min^{-1}.

3. Result and discussion

3.1. Determination of the microemulsion compositions from the sketch phase diagram

To our knowledge, the microemulsion is a thermally stable and transparent system. The titration method was used to determine the reverse microemulsion region on base of the variation from transparence to opaque. The transparent single-phase microemulsion regions are shown in shady regions in Fig. 1. Compared to $Cd(NO_3)_2$-containing microemulsion, the single-phase region of the NH_4OH-containing reverse microemulsion was narrower, indicating the solubility of the NH_4OH solution in oil phase was small. It was probably that the competitive combination of OH^- and NH_3 with water molecules prevented from the hydrogen-bonds formation between water and surfactant molecules. As a result, the solubility of the water decreased greatly. Kon-no and Kitahara [24] and Fang [25] also reported the similar results. Kon-no and Kitahara have reported that the solubility of water was affected predominately by the anions other than the cations. Fang further demonstrated that the microemulsion region would become narrower when the alkali concentration increased. In addition, with increasing of the surfactant concentration, the microemulsion region areas first increase and then decrease. The former is easy to understand, which benefits to the formation of the stable microemulsion; the latter is probably due to the appearance of the liquid crystal phase. In order to ensure the system stable, the microemulsion system, which the point C in Fig. 1 represented, was used to prepare the particles.

3.2. Size control of the CdS cores

Size of the CdS core was controlled through tuning the addition amount and the addition way of the reactants. In order to prepare small CdS cores, ME-1 was mixed directly with ME-2 with equal volumes under stirring vigorously. The Na_2S- and $Cd(NO_3)_2$-containing micelles collided and associated. During the process, the matter exchanged simultaneously. The reactants reacted, nucleated and grew within the reverse micelles. Because of the protection of the interface film, the conventional agglomeration of the particles could be effectively refrained. The monodispersed particles could be obtained. Table 2 presents the preparation conditions of the samples. The CdS cores with average 5 nm in diameter were prepared (Sample 1 in Table 2 and Fig. 2a) by mixing directly 5 ml ME-1 and 5 ml ME-2.

Seeding growth procedure was conducted to obtain the large cores. Small amount of ME-1 and ME-2 were first

Table 2
The preparation conditions of the CdS–SiO_2 core-shell composites

Sample	ME-1 (ml)	ME-2 (ml)	ME-3 (ml)	TEOS (g)	Particle size (nm)
1	5	5	10	1.0	35
2	5 + 5	5 + 5	20	4.0	50
3	10 + 10	10 + 10	20	4.0	100
4	10 + 30	10 + 30	30	10.0	1500

ME-1: $Cd(NO_3)_2$-containing microemulsion; ME-2: Na_2S-containing microemulsion; ME-3: NH_4OH-containing microemulsion; TEOS: $Si(OEt)_4$.

mixed under stirring. After the small seeds were stabilized for a time, a definite amount of ME-1 and ME-2 were added alternately to make the small cores grow into the desired large ones. During the process, the initially formed CdS nanocrystals might act as the growth seeds, which provided with the nucleation and growth sites; the reacting species added subsequently reacted and grew on the seed surface into large crystals. Observed from Table 2, Figs. 3 and 5, the core size of Samples 1, 2, 3, and 4 are 5, 8, 50, and 1200 nm, respectively. The results showed that the core size could be controlled precisely by altering the addition amount and the addition way of the reactants.

3.3. Control of the SiO_2 shell thickness

The shell thickness of the CdS–SiO_2 composites particles could be controlled simply by altering the addition amount of TEOS. After the CdS cores formed, ME-3 was added under stirring. Then, a definite amount of TEOS was added dropwise to hydrolyze and polymerize. Note that the TEOS reaction was much slower in the microemulsion than that in the Stöber process [26,27]. Therefore, aging for 24 h was required during the process. In the process, similar to the secondary seeding growth procedure above, TEOS hydrolyzed and polymerized on the CdS core surface. The CdS cores could provide with nucleation and growth sites for the silica, and the silica shell of different thickness formed. Shown in Fig. 3, Fig. 5 and Table 2, the shell thickness of the Samples 1, 2, 3 and 4 are 15, 20, 25 and 100 nm, respectively. More interestingly, the microparticles were also obtained in this process (Sample 4). In addition, sometimes several cores were contained in one composite particle; however, it was not found that the particles without cores or without shell were formed. Observed from Fig. 3, the CdS–SiO_2 particles are

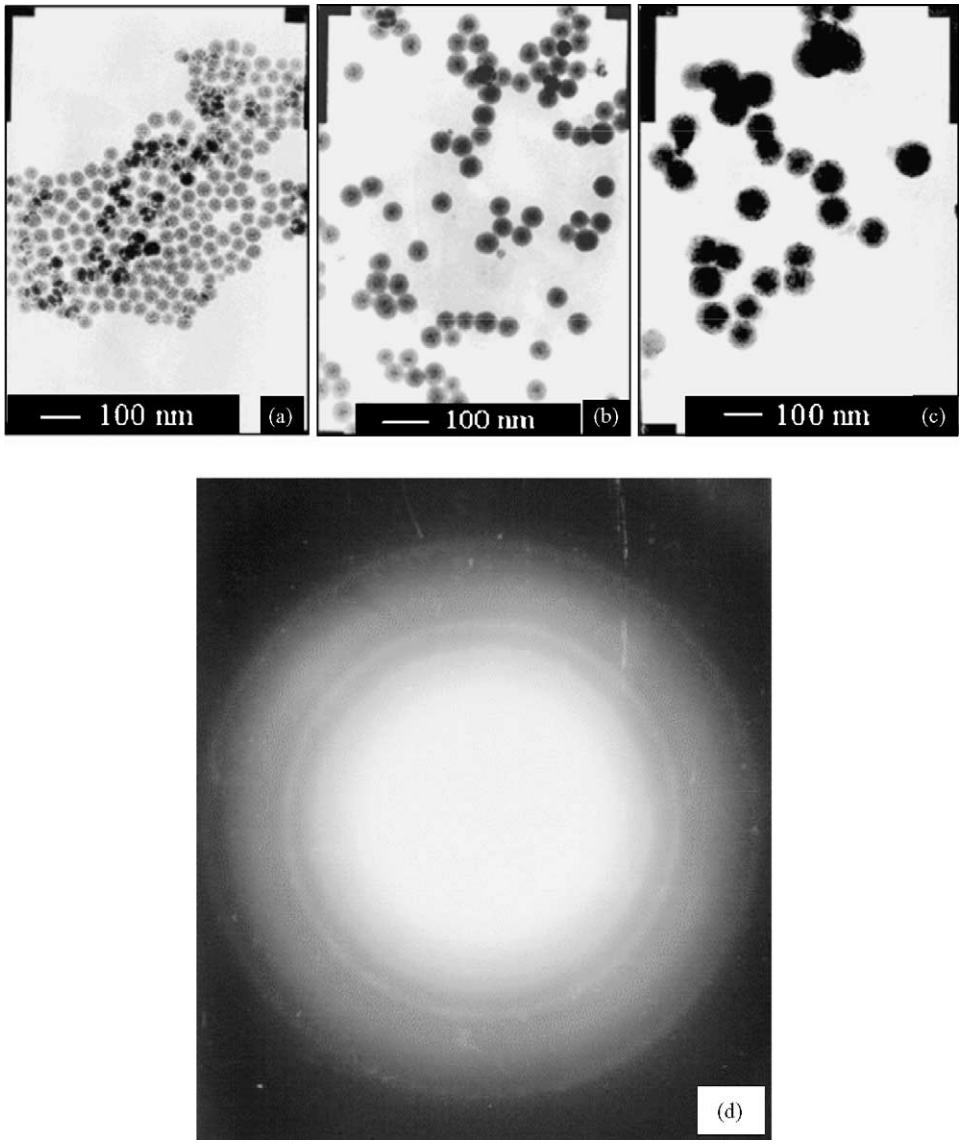

Fig. 3. Transmission electron micrographs of CdS–SiO_2 core-shell nanocomposites (a) Sample 1, (b) Sample 2, (c) Sample 3, (d) SAED patterns of Sample 2.

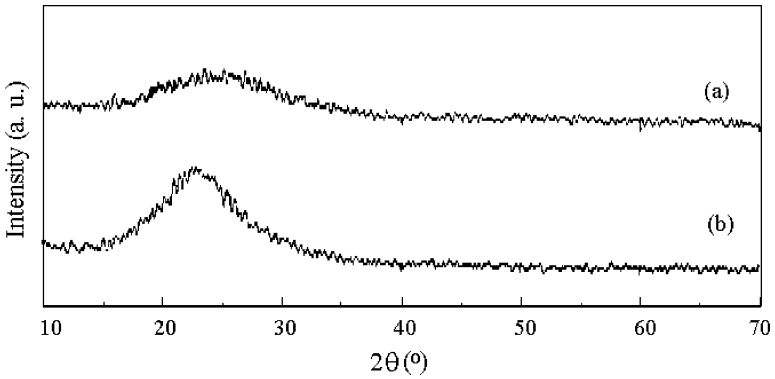

Fig. 4. XRD patterns of the Sample 2 before and after being treated with nitric acid (a) CdS–SiO_2; (b) Hollow SiO_2.

uniform, and the standard deviation of the particle size distribution is less than 5% (calculated from 100 particles), which indicates the size distribution of the CdS–SiO_2 particles could be controlled well by the microemulsion technique.

Typically, Sample 2 was further characterized with XRD and SEAD to investigate crystalline phase of the CdS core. Fig. 4 shows the XRD patterns for the Sample 2. No characteristic diffraction peaks of CdS crystal appeared, and only a very wide peak was observed at $2\theta = 20$–27°, identified as amorphous silica. An attempt to characterize the CdS–SiO_2 sample by XRD was not successful, because no characteristic diffraction peaks of CdS crystalline were observed. The result might be related to the small size of the sample. However, the crystalline phase present in the CdS–SiO_2 sample could be confirmed by selected area electron diffraction (SAED) performed on the CdS–SiO_2 nanocomposites (shown in Fig. 3d). The characteristic diffraction rings of CdS crystalline were observed clearly, indicating the CdS cores exhibited polycrystalline structure. The SAED patterns of the sample consisted of a few relatively broad diffuse rings, which resulted from its very small dimensions. The broad rings indicated a very small grain size. Although the broadening of the rings precluded accurate measurement of lattice spacings, the patterns were found to be more in agreement with the hexagonal phase. Considering the camera constant, which was previously established for exactly the same diffraction conditions, the three prominent rings corresponded satisfactorily to the 100, 110 and 200 reflections of hexagonal CdS. In conclusion, two probably reasons could be concerned for the phenomena above. One might result from diffuse effect (i.e. fringing field effect) of nanocrystals because of there very small size (8 nm). On the other hand, the intensities of the diffraction peaks decreased greatly because of the very small loading amount of the CdS cores in the sample, which might be beyond the effective detection limit of the XRD instrument.

3.4. Evaluation of the hollow SiO_2 spheres

After the CdS–SiO_2 core-shell composites were treated with nitric acid, the hollow SiO_2 spheres were obtained accordingly. It was interesting that the hollow SiO_2 spheres retained the same size and morphologies as the CdS–SiO_2 core-shell particles. Fig. 5a shows the hollow SiO_2 spheres obtained from Sample 2. Comparing Fig. 5a with Fig. 3b, the CdS cores were removed completely. Because the CdS core possesses higher electron density than the SiO_2 shell, the TEM images of the CdS cores in the CdS–SiO_2 samples are observed clearly. After being treated with the nitric acid, the deep black cores (CdS) disappeared, indicating that CdS cores were eliminated indeed. This could be also demonstrated by the color variations of the sample before and after

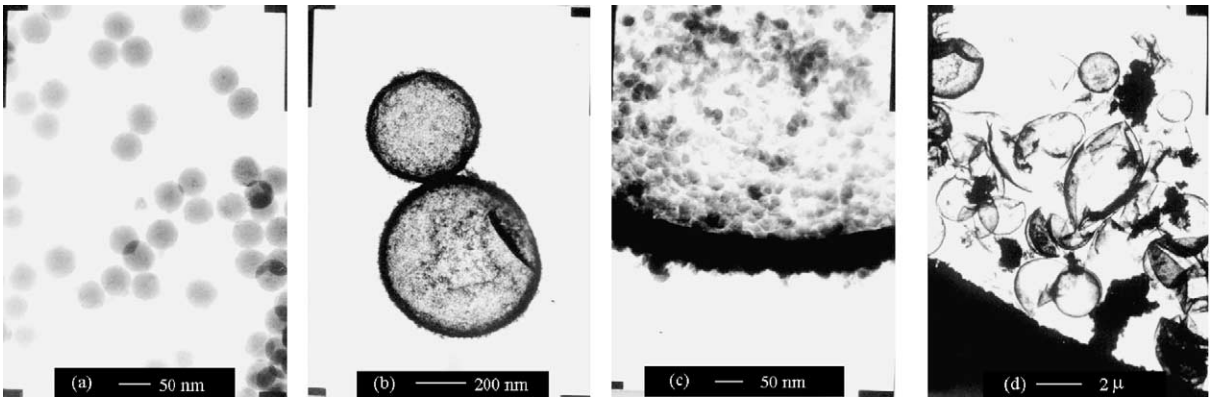

Fig. 5. Transmission electron micrographs of hollow SiO_2 spheres (a) Sample 2; (b) Sample 4; (c) Shell of Sample 4; (d) deliberately broken hollow sphere of Sample 4.

Table 3
Surface areas and XRF element analysis of CdS–SiO_2 composites and hollow SiO_2 spheres

Sample	Cd/Si (mol%)		SSA ($m^2\ g^{-1}$)	
2	3.3[a]	0[b]	103.1[a]	191.8[b]
4	4.1[a]	0[b]	62.3[a]	150.0[b]

a: before washed with nitric acid; b: after washed with nitric acid; SSA: specific surface area.

treatment with nitric acid. Since CdS and SiO_2 are yellow and white, respectively, it was clearly observed that the color of the sample changed from yellow to white after treatment with nitric acid. Another forceful proof was the results of XRF element analysis (Table 3). It was quantitatively determined by XRF element analysis that the ratios of Cd to Si before and after treatment were 4.1 and 0 mol%, respectively. However, we cannot determine from Fig. 5a whether the silica spheres were hollow or not, because the interior voids are not obvious. This could be ascribed to the CdS cores, which were too small. The presence of the voids could be supported by the results of N_2 adsorption. It was well known that the particle surface area was mainly provided by silica. If the voids were present, the surface area would increase obviously. Table 3 shows that the surface area of the Sample 2 increased from 103.1 to 191.8 $m^2\ g^{-1}$ after being treated with nitric acid, which demonstrated forcefully the formation of hollow silica sphere.

For the hollow SiO_2 microspheres, the presence of the voids was very obvious. Observed from Fig. 5b and c, the hollow SiO_2 microspheres have a cavity of 1.2–1.8 μm in diameter and shell of 80–100 nm in thickness. The deliberately broken experiment also proved that the SiO_2 microspheres were hollow indeed (shown in Fig. 5d). N_2 adsorption analysis showed that after treatment with nitric acid, the surface areas of Sample 4 increased from 62.3 to 150.6 $m^2\ g^{-1}$, which proved forcefully that the microspheres are hollow.

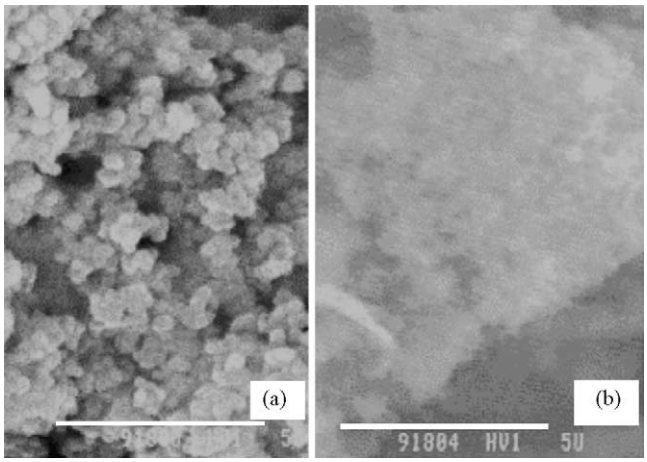

Fig. 6. Scanning electron micrographs of hollow SiO_2 spheres (a) Sample 2; (b) SiO_2 shell of Sample 4.

The surface of the hollow SiO_2 spheres was further observed with SEM. Fig. 6a shows that the surface of the uniform hollow nanoparticles was slippery, indicating that the nanosized particles probably were formed within the reverse micelles. However, Fig. 6b shows that the surface of the Sample 4 was coarse, which consisted of the nanosized particles. This indicated a formation mechanism for the microspheres, differing from the nanoparticles, which probably formed through the aggregation of the nanoparticles.

3.5. The proposed formation mechanism of the particles

The probably formation mechanisms of the hollow nano- and micro-spheres were proposed and shown in Fig. 7. It was proposed that the formation mechanism probably in-

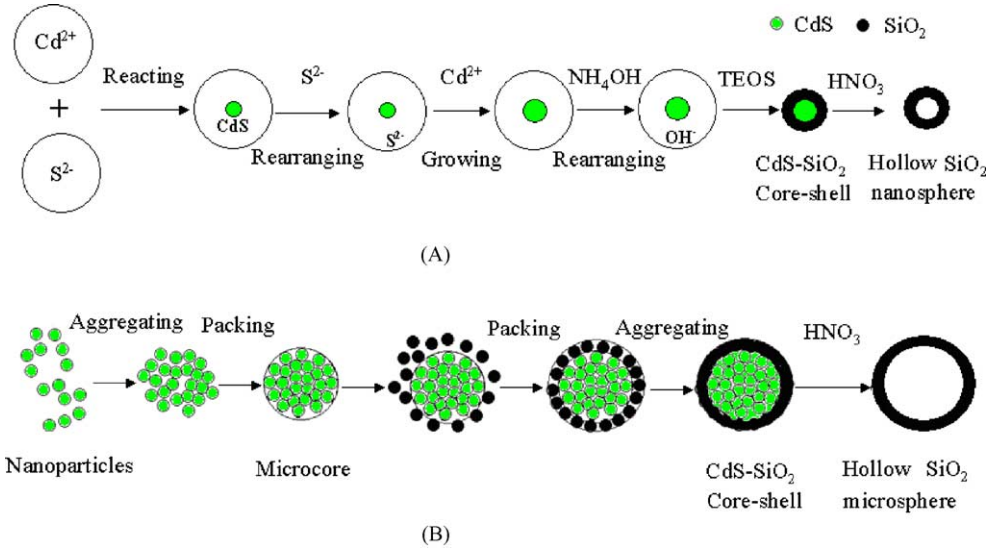

Fig. 7. Formation processes of CdS–SiO_2 composites and hollow SiO_2 spheres (A) the formation process of nanoparticles; (B) the formation process of microspheres.

volved two processes. The first process was the formation of nanoparticles controlled by reverse micelles, shown in Fig. 7A. The nucleation and growth processes were confined within the "water pool", which benefited to the formation of uniform nanoparticles. The second was the self-assembly of the nanoparticles through a closely packing process, shown in Fig. 7B. Under surface tension or/and van der Waal force, the microspheres were formed through the aggregation and packing closely of the formed nanoparticles [28,29].

4. Conclusion

In conclusion, the monodispersed CdS–SiO_2 core-shell particles and hollow SiO_2 spheres ranging from nanometers to microns could be prepared in the reverse microemulsions. The nucleation, growth and aggregation processes could be controlled by the microemulsion. The core size and shell thickness could be tuned easily by controlling the addition amount and addition ways of the reacting species. The CdS–SiO_2 core-shell composites could be further used to synthesize advanced functional materials through grafting other functional molecules on the surface of composites, and the hollow silica sphere could be potentially used as useful supports of catalysts because of their high surface area. Extensive study is focusing on the applications of the materials.

Acknowledgements

The financial support from the Ministry of Science and Technology of the People's Republic of China is gratefully acknowledged (G1999022401).

References

[1] F. Caruso, R.A. Caruso, H. Möhwald, Science 282 (1998) 1111.
[2] R. Davies, G.A. Schurr, P. Meenan, R.D. Nelson, H.E. Bergna, C.A.S. Brevet, R.H. Goldbaum, Adv. Mater. 10 (1998) 1264.
[3] G. Oldfield, T. Ung, P. Mulvaney, Adv. Mater. 12 (2000) 1519.
[4] F. Caruso, Adv. Mater. 13 (2001) 11.
[5] M. Giersig, T. Ung, L.M. Liz-Marzan, P. Mulvaney, Adv. Mater. 9 (1997) 570.
[6] T. Chen, P. Somasundaran, J. Am. Ceram. Soc. 81 (1998) 140.
[7] T. Torimoto, J.P. Reyes, K. Iwasaki, B. Pal, T. Shibayama, K. Sugawara, H. Takahashi, B. Ohtani, J. Am. Chem. Soc. 126 (2003) 316.
[8] Rohm, Haas, US Patent 4,427,836 (1984).
[9] M. Ramanurti, K.H. Leong, J. Aerosol Sci. 18 (1987) 175.
[10] D.E. Bergbreiter, Angew. Chem. Int. Ed. 38 (1999) 2870.
[11] S.Y. Chang, L. Liu, S.A. Asher, J. Am. Chem. Soc. 116 (1994) 6739.
[12] A.R. Kortan, R. Hull, R.L. Opila, M.G. Bawendi, M.L. Steigerwald, P.J. Carroll, L.E.J. Brus, Am. Chem. Soc. 112 (1990) 1327.
[13] K. Dick, T. Dhanasekaran, Z.Y. Zhang, D. Meisel, J. Am. Chem. Soc. 124 (2002) 2312.
[14] M. Bruchez Jr., M. Moronne, P. Gin, S. Weiss, A.P. Alivisatos, Science 281 (1998) 2013.
[15] H. Mattoussi, J.M. Mauro, E.R. Goldman, G.P. Anderson, V.C. Sunder, F.V. Mikulec, M.G. Bawendi, J. Am. Chem. Soc. 122 (2000) 12142.
[16] X.H. Fang, X. Liu, S. Schuster, W. Tan, J. Am. Chem. Soc. 121 (1999) 2921.
[17] W.C. Chan, S. Nie, Science 281 (1998) 2016.
[18] Gy. Tolnai, F. Csempesz, M. Kabai-Faix, E. Kálmán, Zs. Keresztes, A.L. Kovács, J.J. Ramsden, Z. Hórvölgyi, Langmuir 17 (2001) 2683.
[19] W. Stöber, A.J. Frink, Colloid Interf. Sci. 26 (1968) 62.
[20] C.-L. Chang, H.S. Fogler, Langmuir 13 (1997) 3259.
[21] F.J. Arriagada, K. Osso-Assare, Colloid Surf. A: Physicochem. Eng. Aspect 154 (1999) 311.
[22] F.J. Arriagada, K. Osso-Assare, J. Colloid Interf. Sci. 211 (1995) 210.
[23] F.J. Arriagada, K. Osso-Assare, J. Colloid Interf. Sci. 170 (1995) 8.
[24] K. Kon-no, A. Kitahara, J. Colloid Interf. Sci. 34 (1970) 221.
[25] J. Fang, Processing of functional ceramics via microemulsion routes, Microemulsion system for producing ultrafine materials, Ph.D. Thesis, National University of Singapore, 1998, Chapter 3.
[26] C. Chang, H.S. Fogler, AIChE J. 42 (1996) 3153.
[27] F.J. Arriagada, Synthesis of submicron particles in reverse micellar systems: nanosize silica via hydrolysis of tetraethoxysilane, Ph.D. Thesis, Pennsylvania State University, 1991.
[28] N. Manoharan, T. Elsesser, J. Pine, Science 301 (2003) 483.
[29] A. van Blaaderen, Science 301 (2003) 470.